This paper is part of the Proceedings of the 14th International Conference on Simulation and Experiments in Heat Transfer and its Applications (HT 2016)
www.witconferences.com

Fibre-based temperature measurement (DTS) in coil-wound heat exchangers for LNG production

R. Hoffmann, R. Flüggen, C. Richardt, J. Ferstl,
C. Kerber & K. Braun
Linde Engineering, Germany

Abstract

Liquified Natural Gas (LNG) is produced using large coil-wound heat exchangers. The heat exchanger performance depends significantly on the spatial distribution of the resulting two-phase flow. Distributed Temperature Sensing (DTS) using optical fibres was used to measure the flow distribution. Initially DTS was qualified in lab tests with respect to the achievable measurement accuracy both at standard temperatures and cryogenic temperatures. Then both a full-scale and a pilot-scale heat exchanger were produced with multi-layer coil-wound fibres integrated in the production process. The full-scale plant was used to monitor performance during commercial LNG production. The pilot-scale plant was used for an experimental series to analyse the heat exchanger performance at different operational states, e.g. applying different distributions to the shell side. The results from the experimental campaign were used to improve and validate an in-house computational model for calculating heat exchanger flow and performance.
Keywords: DTS, coil-wound heat exchanger, LNG.

1 Introduction

Due to the need for non-pipeline-based transport of natural gas an increasing amount of gas is liquefied. Transport is then performed either by ship for inter-continental or inter-regional trade, or by truck.

Liquified Natural Gas (LNG) for intercontinental transport is produced in large liquefaction plants with nameplate capacities between 1 and 10 mtpa (e.g. Hammerfest LNG plant with 4.3 mtpa capacity (see Figure 2)). The feed for these

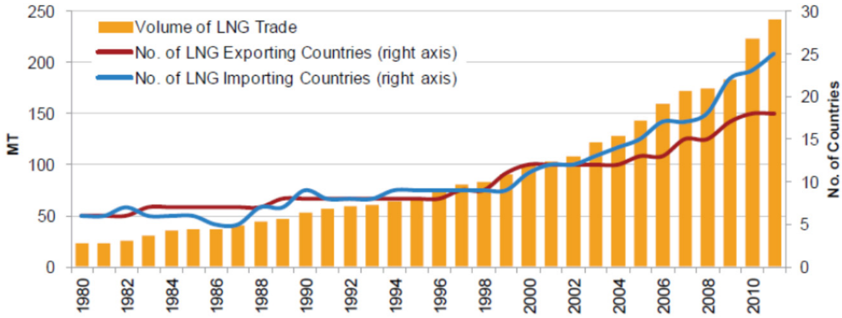

Figure 1: LNG trade volumes 1980–2011 (IGU [1]).

plants is mostly derived directly from a producing gas field. Costly pre-processing of the gas is therefore needed before liquefaction to remove undesirable components like N_2, CO_2, H_2S, water and heavier hydrocarbons. The produced LNG is stored in large flat-bottom tanks with capacities between 100,000 and 1,000,000 m^3.

Figure 2: Hammerfest (Norway) LNG plant.

For mid-sized LNG plants (0.2 to 2.0 mtpa LNG) Linde has devised a single mixed-refrigerant liquefaction process: LIMUM (Linde multi-stage mixed refrigerant process applying coil-wound heat exchanger) [2].

- The low pressure (LP) mixed refrigerant (MR) is compressed in a two stage centrifugal compressor and partially condensed against cooling water or air.
- The heavy, liquid MR fraction is used in a coil-wound heat exchanger to pre-cool natural gas and to condense the lighter gaseous MR fraction partially.
- This lighter MR fraction is again separated. The heavier fraction serves as liquefaction refrigerant, while the remaining light ends MR fraction sub-cools the liquefied natural gas.

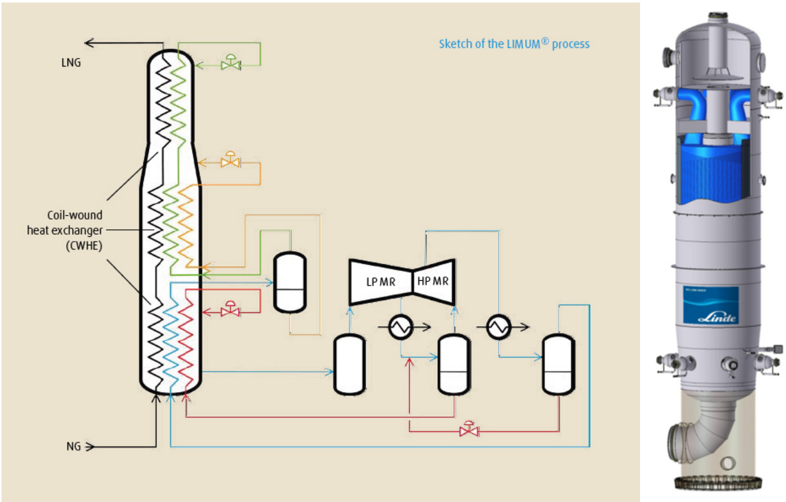

Figure 3: Single mixed refrigerant liquefaction process: LIMUM [2].

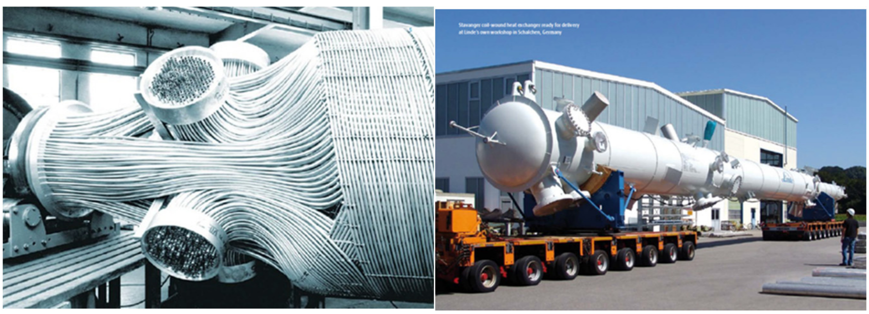

Figure 4: Coil-wound heat exchanger [2].

The central element for the whole process is the coil-wound heat exchanger (CWHE) where LNG – passing through a large number of tubes – is liquefied by the shell side refrigerant due to falling film evaporation. The temperature range is from 30°C to -165°C.

It is difficult to analyse the shell side distribution of the refrigerants liquid phase. However the uniformity of this distribution affects the performance of the CWHE. Thus information about the liquid distribution on the shell side supports the optimization of the CWHE performance.

2 Distributed temperature sensing (DTS)

Information about the liquid distribution on the shell side can be derived from the shell side temperature field. To avoid installing a large number of point temperature sensors fibre-based distributed temperature sensing was used [3, 4].

2.1 Principle

A laser pulse that is injected into an optical fibre is reflected at the quartz structure along the whole fibre length. Physical parameters like temperature or stress influence components of the reflected light. As a result the optical fibre can be employed as a linear sensor.

Depending on various physical effects the light scattered back from the fibre contains different components (Smoken and van der Spek [5]); see Figure 5. The Rayleigh scattering with the wavelength of the laser source used generates the dominant peak. The Raman scattering generates two peaks above and below the Rayleigh peak. The higher peak is the Stokes component which is practically temperature-independent. The lower peak is the temperature-dependent anti-Stokes component. The local temperature of the optical fibre is derived from the ratio of the Anti-Stokes and Stokes light intensities.

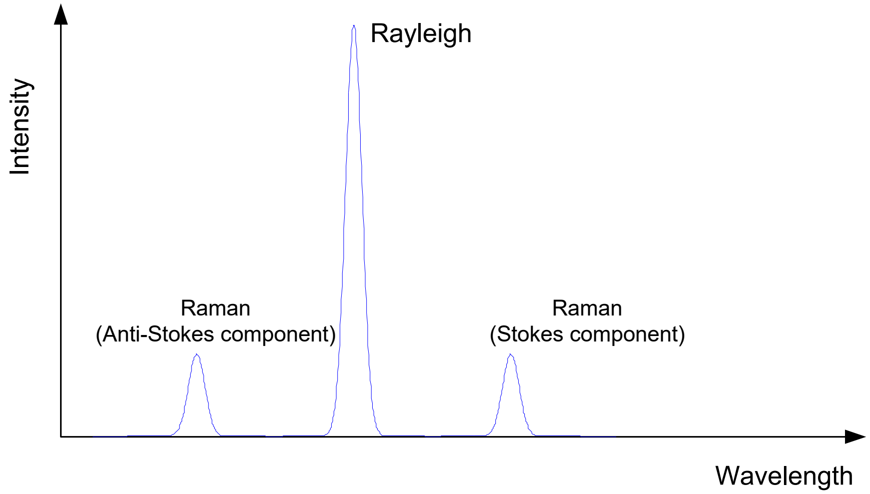

Figure 5: Components of reflected light in an optical fibre.

2.2 Qualification

To qualify the technology measurements were performed at defined temperatures:

- A cryostat filled with Liquid Nitrogen (LIN).
- A refrigeration unit filled with methanol.
- An insulated bin filled with an ice/water mixture.
- A thermostat filled with silicone-oil that was adjusted to three different temperature levels (70°C, 140°C, 210°C).
- A drying oven providing stable temperatures up to 500°C.

Control measurements were performed using calibrated Pt100 thermo elements.

	LIN	Cryostat	Icewater
			
Temperature Level	-196°C	-70°C	0°C
Accuracy (PT100)	±/0.1	± 0.3	± 0.1
Filled with	LIN	Methanol	Water / Ice

Figure 6: Cold measurement environments.

The two most important measurement parameters for a DTS system are the measuring time and the sampling interval. Figure 7 shows the result from a qualification run of a long fibre at a stable temperature of +70°C. The histograms show the measured temperatures along the fibre.

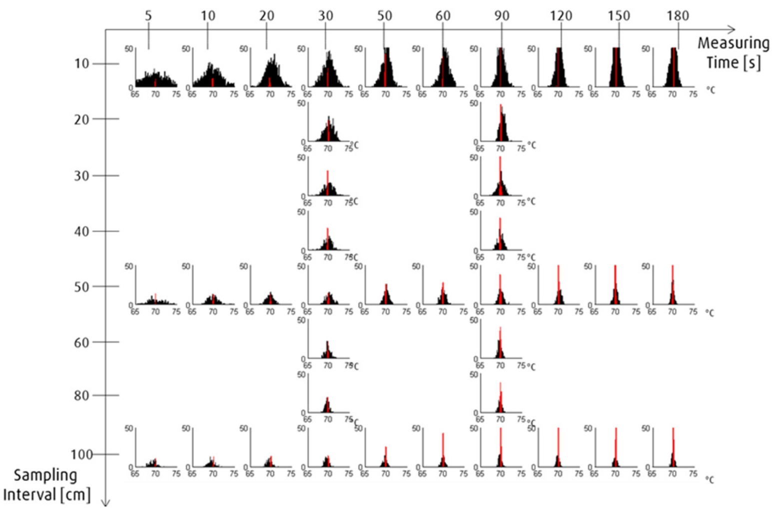

Figure 7: Effect of measuring time and sampling interval.

By increasing the measuring time the signal-to-noise ratio is reduced leading to correspondingly higher measurement accuracy (see Figure 7, top row, for an example with measuring times from 5 seconds to 180 seconds). Increasing the sampling interval in the direction of the fibre leads also to a reduction of signal-to-noise ratio, since the backscattering signal from a longer fibre segment is integrated into a single measurement point. The trade-off for a longer sampling interval is of course the reduced number of measurement points along the whole fibre.

Another important aspect of setting up a DTS measurement system is the need for calibration. Calibration is typically done at a well-defined reference temperature which should be near the measurement temperature. Figure 8 shows the effect of measuring at temperatures far from the calibration temperature (the red histograms indicate the DTS readings, the blue histograms indicate the Pt100 readings): Calibration was performed at +70°C, while measurements were also performed at 0°C, -70°C and -196°C. At 0°C the DTS was still aligned with the Pt100 but at -70°C there was already a difference of 2–3°C. The effect at -196°C was even worse, especially since the backscattered signal level at these low temperatures gets very small, leading to a large standard deviation of the calculated temperature.

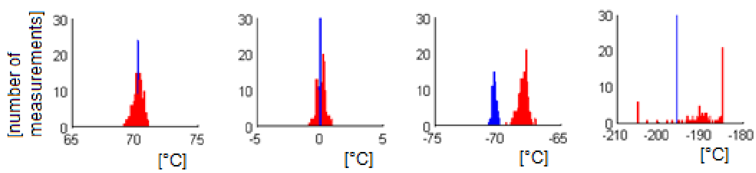

Figure 8: Effect of different calibration and measurement temperature.

2.3 3D Interpolation techniques

A pilot-scale coil-wound heat exchanger (700 mm diameter, 1800 mm height) was built to test DTS monitoring. Three layers of the heat exchanger tubes were supplemented with a fibre embedded in a stainless steel capillary.

Figure 9 shows the geometry of the three fibre spirals (red line), the DTS measurement points along the fibre (blue crosses) and the location of nine Pt100 elements (green circles) that were installed for comparison.

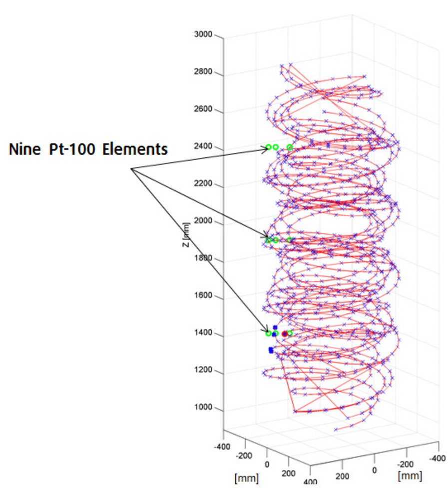

Figure 9: Fibre geometry in pilot-scale coil-wound heat exchanger.

As the fibre temperature measurements are distributed irregularly in space a transformation is needed towards a regularly spaced grid. This is required both for data analysis, display and comparison with the Pt100 sensors.

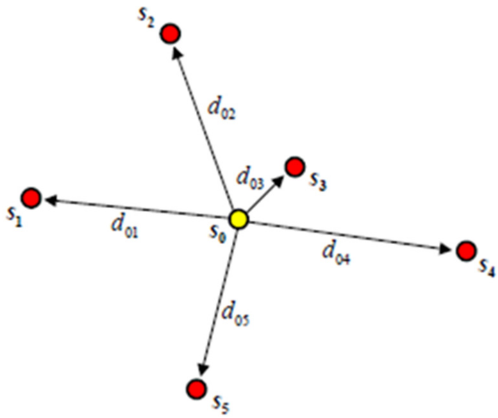

Figure 10: 3D distance-dependent interpolation.

To calculate the temperature $T(s_0)$ at position s_0 the measured temperatures T at the surrounding positions s_i are weighted with a suitable weighting function w and averaged

$$\hat{T}(s_0) = \frac{\sum_{s_i \in S(s_0)} w(d_{0i}) \cdot T(s_i)}{\sum_{s_j \in S(s_0)} w\left(d_{0j}\right)}$$

Interpolation algorithms differ typically in their weighting functions and in the amount of neighbouring measurement values included.

The most straight-forward algorithm is linear interpolation. An alternative technique that is often used is inverse distance weighting, Franke [6]. The weighting function is decreases inversely with the distance from the measurement point so that nearer measurements are weighted stronger. The drawback is that the nearest measurement tends to dominate all other measurements so that any error in that measurement is fully replicated in the interpolation. The advantage of many measurements along the fibre where statistical errors can cancel out each other is thus no longer given.

The algorithm is therefore modified to include an upper and lower cut-off radius. Below the lower cut-down radius the weighting function assumes a value w_{max}. Above the upper cut-off radius the weighting function is set to 0 to reduce the calculation time, since far-away measurements should have only negligible influence on the result.

$$w(d_{0i}) = \begin{cases} w_{max} \; for \; r < r_{min} \\ \frac{1}{r^2} \; \text{for } \mathrm{r}_{min} < r < \mathrm{r}_{max} \\ 0 \; for \; r > r_{max} \end{cases}$$

An alternative to inverse distance weighting is an exponential smoother (Figure 11). It avoids the singularity for small distances and allows an adjustment of its slope by introducing a parameter a

$$w(\boldsymbol{d_{0i}}) = e^{-ar}$$

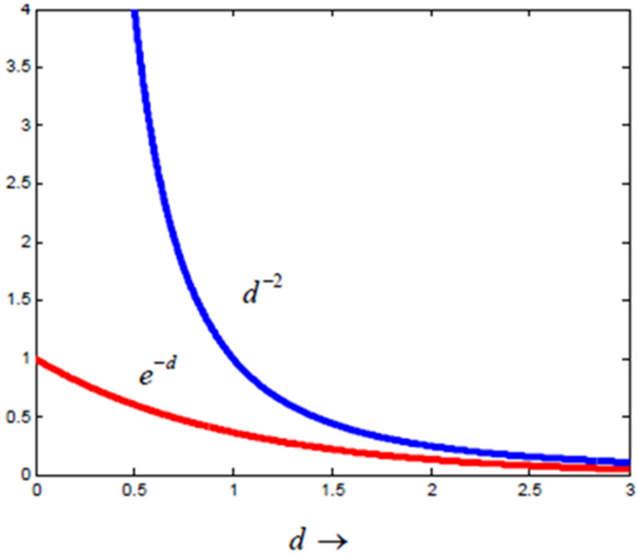

Figure 11: Inverse distance weighting vs. exponential smoother.

It is also possible to introduce different weightings depending on the direction in space, by calculating the distance r as

$$r = \sqrt{b\Delta x^2 + c\Delta y^2 + d\Delta z^2}$$

Figure 12 compares the different interpolation techniques for an experiment were cold liquid refrigerant was fed to only the inner area around the mandrel on top of the heat exchanger. Due to the broad boiling range of the refrigerant, the visible temperature changes indicate the evaporation progress of the liquid component on its way downward through the heat exchanger. As to the comparison of the interpolation techniques:

- The standard *linear interpolation* results in very irregular shapes.
- These irregular shapes can be smoothed by applying a *filter* in a second step. In this case a 2D-gaussian filter was used.
- *Inverse distance weighting* has the problem that it averages over too large areas (thus obliterating the effect of the inhomogeneous liquid injection) while at the same time the marked artefacts appear wherever a measurement was too near an interpolation point. It was not possible to find a combination of cut-off radii that mitigated this problem.
- The *exponential smoother* provided the best results: It not only gave smooth pictures, but resulted also on average in the smallest deviations between Pt100 and fibre measurements.

www.witpress.com, ISSN 1743-3533 (on-line)

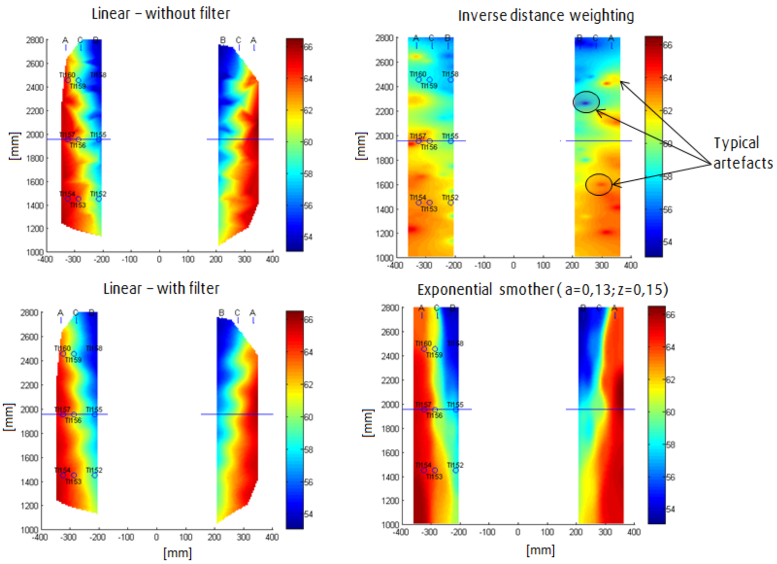

Figure 12: Comparison of different interpolation techniques.

Using the exponential smoother interpolation technique all DTS measurements of the whole campaign were evaluated. In total 37,320 fibre measurements had been performed in this time. The difference between Pt100 and fibre was plotted as a histogram in Figure 13. The mean deviation is -0.304°C and the standard deviation is 0.76°C. 89% of all measurements had a difference below 1°C.

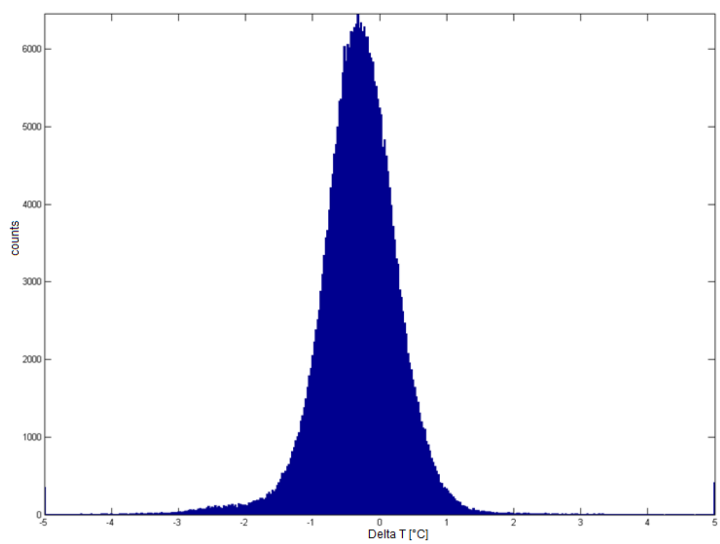

Figure 13: Deviation between all DTS and Pt100 measurements.

www.witpress.com, ISSN 1743-3533 (on-line)

3 Application on a full-scale heat exchanger

The DTS measurement technique was implemented in a base-load LNG plant (0.3 mtpa capacity) near the city of Stavanger, Norway, started-up for commercial production in 2010. Figure 14 shows the coil-wound heat exchanger. Optical fibers with a total length of approx. 3 km were wound together with the coils. At a sampling resolution of 0.5 m roughly 6000 measurement points in the bundle are available. Using the interpolation techniques shown above detailed analysis of the plant performance also in transient conditions like during start-up or shut-down became available.

Figure 14: Stavanger, Norway base-load LNG plant [2].

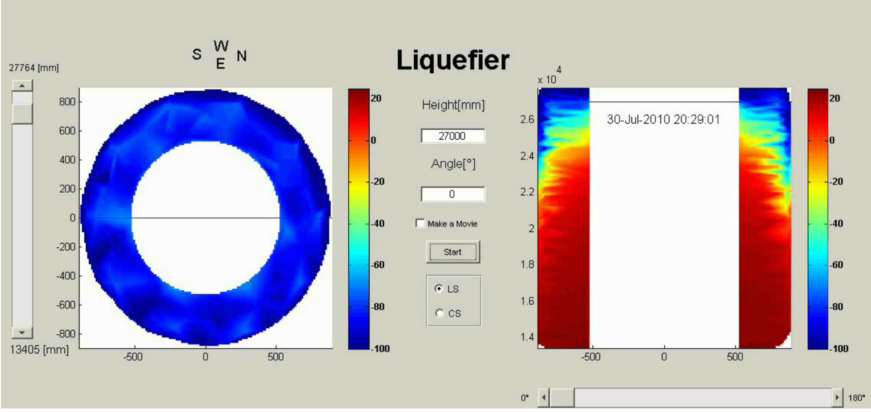

Figure 15: Example of liquefier during start-up (Richardt [7]).

References

[1] Internation Gas Union (IGU), World LNG Report, 2011.

[2] The Linde Group, Baseload LNG Production in Stavanger. http://www.linde-engineering.de/internet.le.le.deu/de/images/LNG_3_3_e_11_150dpi563_15617.pdf.

[3] Abhisek Ukil, Hubert Braendle and Peter Krippner, Distributed Temperature Sensing: Review of Technology and Applications. *IEEE Sensors Journal,* **12(5)**, 2012.

[4] Technology, LIOS. [Online] http://www.lios-tech.com/Menu/Technology.

[5] Smolen, James J. and Alex van der Spek, "Distributed Temperature Sensing." A primer for Oil and Gas Production. Shell, 2003.

[6] Franke, Richard, Scattered Data Interpolation: Tests of Some Methods. *Mathematics of Computation*, **157(38)**, pp. 181-200, 1982.

[7] Richardt, Carsten, Temperature measurement in LNG heat exchangers by means of optical fibers. Achema, Frankfurt, Germany, 2012.

www.witpress.com, ISSN 1743-3533 (on-line)